Barriers to field line transport in 3D magnetic configurations

Barriers to field line transport in 3D magnetic configurations

D Grasso[1,2], D Borgogno[2], F Pegoraro[3], TJ Schep[4]

[1] Istituto dei Sistemi Complessi - CNR, Roma, Italy
[2] Dipartimento di Energetica, Politecnico di Torino, Italy
[3] Phys. Dept. Pisa University, Pisa, CNISM, Italy
[4] Phys. Dept. Eindhoven University of Technology, The Netherlands

E-mail: daniela.grasso@infm.polito.it

Abstract. The transport properties of magnetized plasma configurations are studied that arise from a one-dimensional, current layer that is unstable to reconnecting modes. These magnetic configurations are partially stochastic. It is shown that ridges in the Finite Time Lyapunov Exponents (FTLE) distribution are aligned with the invariant manifolds related to the lines of uniform hyperbolicity. It is shown that these ridges form approximate Lagrangian Coherent Structures (LCS) and act as barriers to the transport of magnetic field lines.

1. Introduction

In this paper we study the spatial topology of 3D magnetic configurations with a strong background magnetic field. Such configurations will be a mixture of volumes where the field is regular and the field lines form periodic or quasi-periodic trajectories, and volumes where the field is irregular and the trajectories are chaotic. The standard tool for analyzing such structures is the method of Poincaré sections in which the field equations are integrated for sufficiently large values of the parameter along the field lines that plays the role of an effective-time and one starts from many initial conditions. Although this technique is rather powerful, it has some serious limitations. In the first place it is limited to periodic or quasi-periodic systems and cannot deal with fully 3D systems. In the second place, Poincaré plots will not tell you where and to what degree a system becomes chaotic so that it does not provide information on the transport process that characterize the transition from local to global chaos.
The magnetic field is represented by

$$\mathbf{B} = B_0 \mathbf{e}_z + \mathbf{e}_z \times \nabla \Psi, \tag{1}$$

where the strong background field B_0 is constant and normalized to unity, and $\Psi = \Psi(x, y, z, t)$ is the poloidal magnetic flux function, which varies in time under a reconnection process.
At each time t the trajectory $\mathbf{x}(z; z_0, \mathbf{x}_0)$ of the magnetic field passing through $x(z_0) = \mathbf{x}_0$, obeys the Hamiltonian system

$$\frac{dx}{dz} = -\frac{\partial \Psi}{\partial y}, \qquad \frac{dy}{dz} = \frac{\partial \Psi}{\partial x}. \tag{2}$$

These equations describe a dynamical system moving in field line time z in the $(x,\ y)$ plane in the presence of a flow field with components $(-\Psi_y, \Psi_x)$.

The system is integrable if the flux function does not depend on the field-line-time, i.e., the axial coordinate z. Then, the elliptic and hyperbolic points of (2) are the solutions for which its right-hand vanishes.
At a hyperbolic point (X-point) lines emanate, the separatrices, that form the stable and unstable manifolds associated with the hyperbolic point. These manifolds, curves in the $(x,\ y)$ plane in the 2D context, are invariant surfaces that separate topologically different type of field lines, i.e., they separate regions with closed field lines from regions with open field lines.
Perturbations that are z-dependent will destroy the integrability. The position of an X-point, i.e. a point where the gradient of the flux function vanishes, will also be z-dependent. The path that is traced out by such a point is, however, not a solution of Eq.(2). This means that in 2D motions with arbitrary z-dependence, the trajectory of the "instantaneous" X-point of the field is not a hyperbolic trajectory and no invariant surfaces are related with it! Nevertheless, there exist hyperbolic trajectories in 3D phase-space (x, y, z) that are the generalizations of the 2D hyperbolic points. Such a trajectory *is* a solution of the equations of motion and, thus, a field line. It has the property that all neighboring field lines approach this trajectory exponentially either forward or backward in 'time' z ([1, 2, 3, 4]). It also means that the largest associated Lyapounov exponent is real and positive. The invariant manifolds associated with these trajectories, are the generalizations of the 2D separatrix surfaces, and play an essential role in the topology of magnetic fields.
The stable and unstable manifolds cannot intersect themselves, but they can intersect each other. The intersections of the unstable and stable manifolds of the same hyperbolic trajectory form homoclinic tangles, which determine the local transport. Intersections between a stable (unstable) and an unstable (stable) manifold belonging to different hyperbolic trajectories form heteroclinic tangles. These govern the global transport between nearby chaotic layers. The transition between regular and chaotic configurations was studied in [5] in terms of the field-line-time it takes for heteroclinic intersections to appear.

Although the invariant manifolds contain essential information on the transport properties of the system, a drawback of this method is that these invariant surfaces become so densely folded that they are impossible to trace for sufficiently long times such that their intersections become numerically visible. A consequence is that it is impossible to quantify transport on this basis. Therefore, it might be rewarding to settle for a less exact method and to define transport on the basis of approximate, asymptotic properties of the system.
In this article, we base our investigations on the properties of the field of the Finite Time Lyapunov Exponent (FTLE). The largest positive FTLE measures the exponential separation between two neighboring field lines after a given interval of field-line-time. As will be discussed, this field exhibits clear ridges that form approximate Lagrangian coherent structures (LCS). It is argued that these LCS's play a decisive role in the transition from local to global chaos. During this phase, these hidden coherent structures in the developing chaotic sea, attract field lines and act as barriers to transport of magnetic field lines. The properties of transport between regions separated by such barriers are the subject of this paper. As far as we know this is the first time that the FTLE properties are used to describe chaotic magnetic fields in the context of fusion plasmas.
The paper is organized as follows. Section 2 describes the model and the chaotic system that is generated by a collisionless reconnection event; section 3 describes the LCS we find in this chaotic configuration; section 4 shows why these LCS can be interpreted as transport barriers. We conclude in section 5.

2. 3D chaotic magnetic configuration

We generate a chaotic magnetic field by means of a collisionless reconnection process, extensively described in [6]. We recall here its main features. The two-fluid model derived in [8] is adopted. In this model the reconnection of magnetic field lines is permitted by considering the effect of the electron inertia in Ohm's law, which takes into account also electron pressure gradient effects. The model is valid in the presence of a strong guide field. The model equations are solved numerically in a $3D$-periodic slab geometry starting from a static equilibrium configuration with a one-dimensional shear magnetic field. The spontaneous reconnection process is induced by the onset of multiple helicity perturbations in a configuration with large values of the linear stability parameter Δ'. We consider a configuration with background toroidal and poloidal magnetic fields such that a resonant mode is excited at each of two neighboring surfaces.

The magnetic flux function consists of an equilibrium part $\psi_{eq}(x)$ and a wave-like contribution $\psi(x, y, z; t)$,

$$\Psi(x, y, z, t) = \psi_{eq}(x) + \psi(x, y, z; t), \tag{3}$$

where $\psi(x, y, z; t)$ may be written as a sum over perturbations with different helicities

$$\psi(x, y, z; t) = \Sigma_i \psi_i(x, k_{yi}y + k_{zi}z, t). \tag{4}$$

with $k_{yi} = 2\pi m_i/L_y$, $k_{zi} = 2\pi n_i/L_z$.

The surfaces $x = x_{si}$ where the modes are resonant are characterized by $\mathbf{B}_{eq} \cdot \nabla\Psi = 0$, which yields

$$\frac{d\psi_{eq}(x)}{dx} = -\frac{\partial\psi_i/\partial z}{\partial\psi_i/\partial y} = -\frac{k_{zi}}{k_{yi}}. \tag{5}$$

where $k_{yi} = 2\pi m_i/L_y$, $k_{zi} = 2\pi n_i/L_z$ with $L_y = 4\pi, L_z = 32\pi$.

The numerical simulations were carried out in a triple-periodic slab, with size $L_x = 2\pi$, $L_y = 4\pi$, $L_z = 32\pi$, starting from an equilibrium configuration with magnetic flux function $\psi_{eq} = 0.19\cos(x)$. The initial perturbation consists of two unstable contributions, ψ_1 and ψ_2, with different helicities

$$\psi(x, y, z; t) = \hat{\psi}_1(x, t)\ \exp(ik_{y1}y + ik_{z1}z) + \hat{\psi}_2(x, t)\ \exp(ik_{y2}y + ik_{z2}z). \tag{6}$$

The functions $\hat{\psi}_{1,2}(x, t)$ are chosen so as to approximate the analytic solutions of the linearized dynamical equations. The wave numbers (m_i, n_i) of the two components of the perturbation are $(1, 0)$, for $i = 1$, and $(1, 1)$, for $i = 2$. The amplitude $\hat{\psi}_1$ is of order 10^{-4} and is ten times bigger than $\hat{\psi}_2$.

In the small amplitude linear phase, when the two helicities evolve independently from each other, each mode induces a magnetic island chain around its resonant surface $x = x_{si}$, where $\mathbf{B}_{eq} \cdot \nabla\Psi = 0$. For the case we present here $x_{s1} = 0, \pi$ and $x_{s2} = 0.71, \pi - 0.71$. We remark that resonant surfaces with $x_s > \pi/2$ are simply due to the periodicity of the magnetic equilibrium ψ_{eq}. Since we are interested in the interaction between different helicities, hereafter we we will focus on the magnetic field structure in the reduced interval $-\pi/2 < x < \pi/2$.

When the magnetic islands are sufficiently large to interact with each other, the nonlinear phase of the process enters. Modes with different helicities and higher order modes of the same helicities of the initial perturbation are generated. At this stage the magnetic field topology exhibits volumes where field lines are stochastic and whose extension tends to spread during the evolution of the reconnection process [6].

Here we will not deal with the dynamic evolution of the magnetic field, but we will focus on investigating the transport properties of magnetic field lines at a particular fixed value in real time, chosen just before the transition to global chaos.

3. FTLE ridges and LCS

The solution to (2) for the maximum value of the distance $||\delta\mathbf{x}(z)||$ between two neighboring field lines can be written as

$$max\ ||\delta\mathbf{x}(z)|| = e^{\sigma(z,z_0,\mathbf{x}_0)|z-z_0|}\ ||\delta\mathbf{x}(z_0)|| \tag{7}$$

where $||\delta\mathbf{x}(z_0)||$ is the initial distance at field-line-time z_0 and σ is defined by

$$\sigma(z, z_0, \mathbf{x}_0) = \frac{1}{|z - z_0|} \ln \sqrt{\lambda(z, z_0, \mathbf{x}_0)}, \tag{8}$$

where $|z - z_0|$ is the length of the effective time at which the FTLE is computed and λ is the largest positive eigenvalue of the tangent map associated with (2)[11]. The square root of λ is the factor by which a perturbation is maximally stretched.

In the infinite time limit $|z - z_0| \to \infty$ the standard Lyapunov coefficient is obtained. While this standard Lyapunov coefficient is constant along each field line, the FTLE is not. In [10] it is shown that

$$\frac{d\sigma(z, z_0, \mathbf{x}_0)}{dz_0} = \mathcal{O}(\frac{1}{|z - z_0|}), \tag{9}$$

so that at long field-line-times, the FTLE becomes a constant.

Within the context of FTLE theory, Lagrangian Coherent Structures may be defined as second-derivative ridges of the scalar FTLE field and following [10] we define a ridge as a curve in the $(x,\ y)$ plane such that the gradient in the FTLE-field is along the curve and such that the second order derivative, given by the Hessian

$$\Sigma = \frac{d^2\sigma(\mathbf{x})}{d\mathbf{x}^2} \tag{10}$$

in the direction perpendicular to the curve is minimal.

In order to extract the ridges in the FTLE field from the magnetic data obtained by the numerical simulations of 3D reconnection processes we developed a new computational algorithm. This solver starts with the computation of the Lyapunov exponents for a set of magnetic field lines at different finite effective-time z according to the method described in [12]. Finite Time Lyapunov exponents for magnetic field line trajectories obtained from both forward and backward time integration of eqs.(2) have to be computed. Forward-time integration, in fact, allows to reveal the repelling branches of the Lagrangian coherent structures, e.g., the unstable manifolds, while in order to locate the attracting patterns, e.g., the stable manifolds, a backward-time integration has to be carried out.

In order to simplify the numerical analysis, controlling in particular the computational time of the FTLE field, we will use approximate descriptions of the Hamiltonian function ψ. As shown in [5], only the higher amplitude modes obtained from the Fourier decomposition of the original data need to be considered, in order to approximate the Hamiltonian accurately. This truncation results in a magnetic flux function with 20 spectral components. For the evolution times considered here it turns out that these latter modes have the helicity of either of the two original perturbations.

As stated in Ref.[13] when ridges are computed using the Hessian of the scalar field, noise amplification can become an issue, especially when chaotic "velocity fields" are taken into account, as in the case of the magnetic fields we considered in this paper. A large collection of criteria addressing ridge filtering is available in technical literature [13]. Here, in order to remove numerical noise effects, we have chosen a natural, easy to implement, criterion which prescribes a minimum height of the ridge. It has be shown that in the case of finite Lyapunov exponent

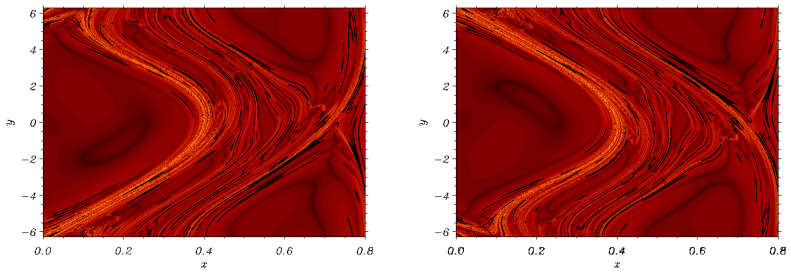

Figure 1. Contour plots of the FTLE computed at $z = 16L_z$ forward (left frame) and backward (right frame) for a set of magnetic field, initially distributed over a uniform 8000×16000 mesh on the domain $0 < x < 0.8$, $-2\pi < y < 2\pi$ of the $z = 0$ section. Superimposed are the ridges extracted by the corresponding FTLE fields.

ridges this leads to significant, consistent, and reliable visualizations [14].
In fig. 1 we show the contour of the FTLE fields evaluated for the dynamical time of the reconnection process we are focusing on and that refers to the local-global chaos transition. The left frame refers to the forward-time integration of the magnetic field line equations, while the right frame refers to the backward-time integration. These FTLE fields have been calculated for a set of $1.28 \cdot 10^8$ magnetic field lines initially distributed at $z = 0$ over a uniform 8000×16000 mesh on the domain $0 < x < 0.8$, $-2\pi < y < 2\pi$.

Figure 1 shows the results after 16 iterations along the toroidal direction. This choice is motivated by a comparison of the results obtained for different integration times. In particular we have carried out simulations up to 20 iterations. Indeed, the essential structures are pretty well represented already after 12 integration times. Superimposed on the contour the corresponding ridges that have been extracted from the FTLE fields are shown in black. These ridges have already been proved in [7] to act as barriers to magnetic field line transport and in the next section we analyze their properties.

4. LCS as transport barriers

In this section we focus on the transport properties of magnetic field lines in the presence of the LCS identified in the previous section. We recall that within the context of a reconnecting system transport of field lines is related with heteroclinic intersections of unstable/stable manifolds with stable/unstable manifolds belonging to different hyperbolic lines, as extensively discussed in [5]. Unfortunately, it is numerically impossible to follow these manifolds sufficiently long in z in order to obtain any realistic estimate of transport based upon heteroclinic intersections. Nevertheless, a comparison of the ridges with the stable and unstable manifolds associated with hyperbolic trajectories show that ridges play the role of magnetic field line transport barriers. This is evident in fig. 2 where we show that the ridges of fig. 1 tend to be aligned with and largely coincide with the initial pieces (*i.e.* evaluated for a few L_z) of the branches of specific stable and unstable manifolds.

In particular, the ridges are shown together with the stable and unstable manifolds associated to the hyperbolic points $(0, -2\pi)$ (green), $(0.51, 0)$ (magenta), $(0.617, 0))$ (light blue), $(0.51827, -1)$ (dark blue), $(0.71, 0)$ (red). The stable and unstable manifolds have been calculated with a Contour Dynamics code [5, 15] only for a few L_z periods. These manifolds are characterized by different frequencies. In particular, we verified that corresponding hyperbolic points have the following periodicities along z: $0L_z$ (green manifold), $5L_z$ (magenta manifold), $3L_z$ (dark blue manifold), $4L_z$ (light blue manifold) and $1L_z$ (red manifold). Since magnetic field lines can not cross these invariant manifolds and since the ridges tend to coincide with the

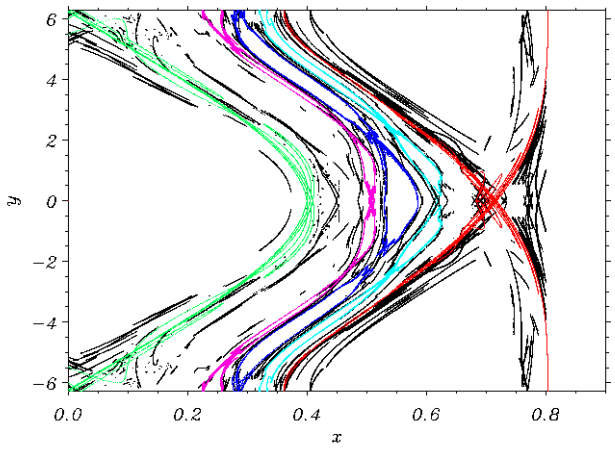

Figure 2. Ridges extracted from the FTLE distribution shown in fig.1 (black curves) with superimposed the corresponding stable and unstable manifolds.

initial part of these manifolds it is expected that these FTLE ridges form barriers with respect to magnetic field line transport.

To quantify how robust these barriers are with respect to the magnetic field line penetration we compare the magnetic topology and the ridges distribution at different effective times in fig. 3. Here the Poincarè plots, obtained for a sample of magnetic field lines initially distributed around a circle centered at the hyperbolic point $(0, -2\pi)$ are overplotted together with the FTLE ridges. We observe that up to $z = 2000L_Z$ the magnetic field lines remain confined by the barrier associated with the magenta manifold. Then up to $z = 7000L_Z$ the confining structure is identified by the barriers associated to the dark blue manifold. After that the relevant confining barriers become the ones associated with the light blue and red manifolds respectively for $z = 12000L_z$ and $z = 20000L_z$. This step-like behavior, where the magnetic field lines remain trapped inside the ridges for finite effective time intervals, is a clear sign of the efficiency of the ridges as barriers.

5. Conclusions

We analyzed the transport properties of a partially chaotic system generated by a collisionless reconnection process, when the transition from local to global chaos occurs. The Lagrangian Coherent Structures that influence the transport of magnetic field lines in this transition phase have been identified by means of the ridges of the Finite Time Lyapunov Exponents. These ridges have been shown to play the role of transport barriers by showing that they partly coincide with the branches of specific stable and unstable manifolds. We observe that the transport of magnetic field line has a step-like behavior. Field lines are at first trapped by the barrier corresponding to the first LCS structures that they encounter in their motion. Then, once they pass this barrier, they spread in a larger volume surrounded by a new barrier and stay there for a second field line time interval. Further in effective time they proceed in the same way until they cross all the barriers and spread over all the chaotic volume.

Acknowledgments

This work was partly supported by the Euratom Communities under the e contract of Association between EURATOM/ENEA. The views and opinions expressed herein do not necessarily reflect those of the European Commission.

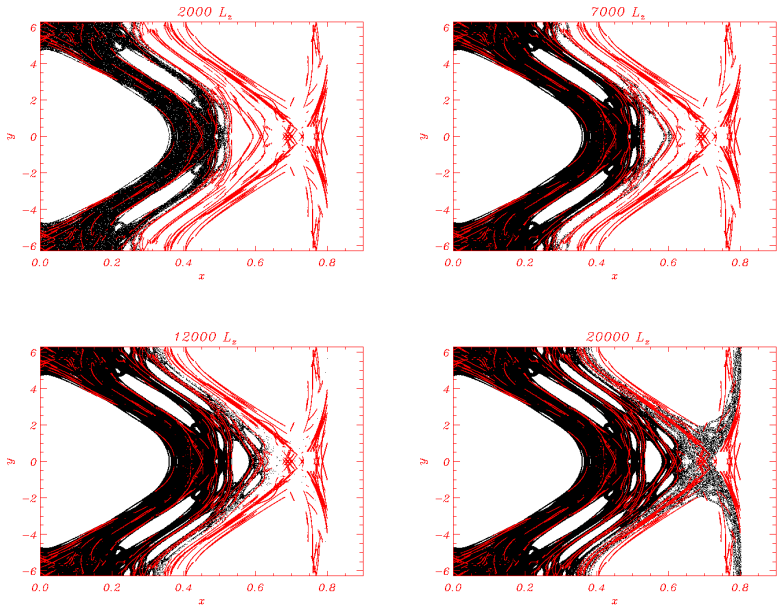

Figure 3. Poincarè maps obtained integrating the field line equations for four different z intervals: up to 2000 toroidal periods (left frame top row), up to 7000 toroidal periods (right frame top row), up to 12000 toroidal periods (left frame bottom row) and up to 20000 toroidal periods (right frame bottom row). Superimposed are the relevant barriers.

References

[1] K. Ide, D. Small, S. Wiggins, *Nonlin. Process.Geophys.*, **9**, 237 (2002).
[2] Ning Ju, D. Small, S. Wiggins, *Int. J. of Bifurcation and Chaos*, **13**, 1449 (2003).
[3] G. Haller, *Chaos*, **10**, 99 (2000).
[4] Ya.B. Pesin, Chapter 7 in *Dynamical Systems II*, Ya. G. Sinai (Ed), Springer Verlag 1989.
[5] D. Borgogno, D. Grasso, F. Pegoraro, T.J. Schep, *Phys. Plasmas.*, **15**, 102308 (2008).
[6] D. Borgogno, D. Grasso, F. Porcelli, F. Califano, F. Pegoraro, F. Farina, *Phys. Plasmas.*, **12**, 032309 (2005).
[7] D. Borgogno, D. Grasso, F. Pegoraro, T.J. Schep, *to be submitted*, (2010).
[8] T.J. Schep, F. Pegoraro, B.N. Kuvshinov, *Phys. Plasmas.*, **1**, 2843 (1994).
[9] G. Haller, Physica D **149**, 248-277 (2001).
[10] S.C. Shadden, F. Lekien, J.E. Marsden, *Phys. D*, **212**, 271-304 (2005); Manikandan Mathur, George Haller, Thomas Peacock, José E. Ruppert-Felsot, Harry L. Swinney, Phys.Rev.Lett. **98**, 144502 (2007).
[11] G. Benettin *et al.*, *Nuovo Cimento* **50 b**, 211 (1979).
[12] G. Rangarajan, S. Habib, R.D. Ryne, *Phys. Rev. Lett.*, **80**, 17 (1998).
[13] F. Sadlo, R. Peikert, *IEEE TRANSACTIONS ON VISUALIZATION AND COMPUTER GRAPHICS* **13**, 6, 1456-1463 (2007).
[14] F. Sadlo and R. Peikert, *Topology-based Methods in Visualization, Mathematics + Visualization*, accepted for publication, 2007.
[15] P.W.C. Vosbeek and R.M.M.Matthey, J.Comput.Phys. **133** 222 (1997).